

## Pu(V) and Pu(IV) Sorption to Montmorillonite

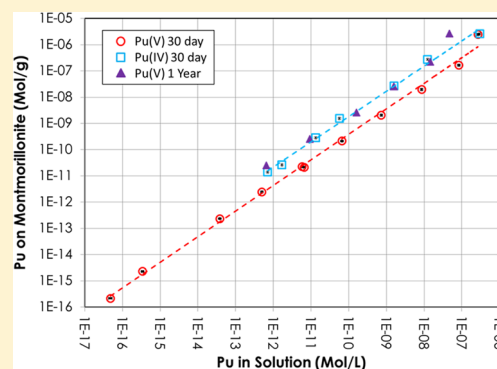
James D. Begg,<sup>\*,†</sup> Mavrik Zavarin,<sup>†</sup> Pihong Zhao,<sup>†</sup> Scott J. Tumey,<sup>†</sup> Brian Powell,<sup>‡</sup> and Annie B. Kersting<sup>†</sup>

<sup>†</sup>Glenn T. Seaborg Institute, Physical & Life Sciences, Lawrence Livermore National Laboratory, Livermore, California 94550, United States

<sup>‡</sup>Environmental Engineering and Earth Sciences, Clemson University, Anderson, South Carolina 29625, United States

### S Supporting Information

**ABSTRACT:** Plutonium (Pu) adsorption to and desorption from mineral phases plays a key role in controlling the environmental mobility of Pu. Here we assess whether the adsorption behavior of Pu at concentrations used in typical laboratory studies ( $\geq 10^{-10}$  [Pu]  $\leq 10^{-6}$  M) are representative of adsorption behavior at concentrations measured in natural subsurface waters (generally  $< 10^{-12}$  M). Pu(V) sorption to Na-montmorillonite was examined over a wide range of initial Pu concentrations ( $10^{-6}$ – $10^{-16}$  M). Pu(V) adsorption after 30 days was linear over the wide range of concentrations studied, indicating that Pu sorption behavior from laboratory studies at higher concentrations can be extrapolated to sorption behavior at low, environmentally relevant concentrations. Pu(IV) sorption to montmorillonite was studied at initial concentrations of  $10^{-6}$ – $10^{-11}$  M and was much faster than Pu(V) sorption over the 30 day equilibration period. However, after one year of equilibration, the extent of Pu(V) adsorption was similar to that observed for Pu(IV) after 30 days. The continued uptake of Pu(V) is attributed to a slow, surface-mediated reduction of Pu(V) to Pu(IV). Comparison between rates of adsorption of Pu(V) to montmorillonite and a range of other minerals (hematite, goethite, magnetite, groutite, corundum, diaspore, and quartz) found that minerals containing significant Fe and Mn (hematite, goethite, magnetite, and groutite) adsorbed Pu(V) faster than those which did not, highlighting the potential importance of minerals with redox couples in increasing the rate of Pu(V) removal from solution.



## INTRODUCTION

The production and testing of nuclear weapons, nuclear accidents, and authorized discharges of radionuclides have all contributed to a global legacy of plutonium (Pu) contamination in the environment.<sup>1–4</sup> Pu mobility in the environment is a topic of key concern because of its radiological toxicity and long half-life (24 100 years for <sup>239</sup>Pu). Due to the health risks of Pu to humans, the EPA has established an extremely low drinking water limit (15 pCi L<sup>-1</sup>/0.55 Bq L<sup>-1</sup>) which is equal to  $1 \times 10^{-12}$  mol L<sup>-1</sup> <sup>239</sup>Pu,  $3 \times 10^{-13}$  mol L<sup>-1</sup> <sup>240</sup>Pu, or  $4 \times 10^{-15}$  mol L<sup>-1</sup> <sup>238</sup>Pu).<sup>5</sup> Despite several decades of study, our understanding of the environmental behavior of Pu is far from complete due to the wide array of factors which can significantly influence its mobility. These include Pu redox processes,<sup>6,7</sup> colloid-facilitated transport processes,<sup>8,9</sup> solubility effects,<sup>10,11</sup> sorption/desorption rates and affinities for natural mineral surfaces,<sup>12,13</sup> and interactions with natural organic matter (including bacteria).<sup>14,15</sup> It has been recognized that colloid-facilitated transport is often a dominant mechanism controlling Pu transport in the subsurface.<sup>8,9,16</sup> Both the formation of Pu oxide colloids (intrinsic colloids) at high concentrations and sorption/desorption of Pu to mineral colloid surfaces (pseudocolloids) are likely to be of environmental significance.<sup>11,13,17</sup> Development of reliable predictive transport models, which are important for risk assessments of both existing contaminated environments and the safety of

long-term disposal of nuclear waste, necessitates a detailed understanding of the stability of Pu associated with colloids (both intrinsic and pseudo).

The oxidation state of Pu strongly affects its environmental mobility. Under typical environmental conditions, Pu can exist in four oxidation states: Pu(III), Pu(IV), Pu(V), and Pu(VI). Pu(III) has been observed under anoxic conditions and in the presence of Fe(II) containing minerals.<sup>7,18,19</sup> Pu(VI) was observed to form in a solubility study at pH 7 with J-13 groundwater from Yucca Mountain under an inert atmosphere, although it has been suggested that it will rapidly reduce to Pu(V) in oxic natural waters.<sup>7,20–23</sup> Pu(IV) and Pu(V) are the more common species under mildly oxic environmental conditions and also represent the oxidation states with the highest (Pu(V)) and lowest (Pu(IV)) predicted subsurface mobilities.<sup>21,22,24</sup>

Several environmentally relevant minerals have been shown to alter the oxidation state of Pu present on their surface although the actual reductant is not always clear.<sup>12,18,19,25</sup> For example, Pu(V) reduction to Pu(IV) has been observed, or inferred, to occur on Mn(II) and Fe(III) minerals as well as

Received: December 21, 2012

Revised: April 12, 2013

Accepted: April 24, 2013

Published: April 24, 2013

silica and montmorillonite.<sup>6,13,17,25–27</sup> Given that these Pu oxidation states exhibit the lowest and highest sorption affinities, respectively, understanding the way in which mineral surfaces control Pu oxidation state is essential to predicting its environmental behavior.

Aluminosilicate clays are ubiquitous in the environment and improving our understanding of Pu sorption to these minerals is important for accurate modeling of actinide transport rates. One common aluminosilicate clay is montmorillonite, a 2:1 dioctahedral smectite and primary component of bentonite. Bentonite is proposed for use within several engineered barrier scenarios for underground nuclear waste repositories.<sup>28</sup> Accordingly, adsorption of Pu to clay minerals is a topic of continued interest.<sup>13,28–30</sup> Montmorillonite is an effective sorbent for a range of metal cations, including Pu.<sup>13,30</sup> Pu(IV)  $K_d$  values from 10 000 to 40 000 mL g<sup>-1</sup> have been reported for smectite-rich sediments in the pH range 5 to 12.<sup>29</sup> Although the high sorption affinity of Pu for montmorillonite suggests the ability of clay minerals to contribute to actinide immobilization (e.g., Pu(V) partitioning to Yucca Mountain tuffs found a ubiquitous and preferential association of Pu with smectite minerals<sup>31</sup>), there are concerns that adsorption to clay minerals may also enhance Pu mobility through colloid-facilitated transport.<sup>8,9,13,16,30</sup>

The adsorption of Pu to smectite minerals has been found to exhibit both pH and ionic strength dependency, indicating that ion-exchange and surface complexation processes may be relevant.<sup>13,28</sup> However, surface complexation will dominate at neutral to alkaline pHs. Surface complexation of metals on clay and other mineral surfaces has often been described in terms of two types of reactive surface sites: “strong sites” which have a high chemical affinity for the metal species and control adsorption behavior at low surface loadings and “weak sites” that become significant at high pH in the presence of high metal concentrations (when the strong sites are saturated).<sup>32–34</sup> The inclusion of two site types is used to account for the observed decrease in sorption affinity as a function of adsorbate concentration (or surface loading).<sup>32,35,36</sup> For example,  $K_d$  values for Np(V) adsorption to goethite have been found to differ by an order of magnitude at solution concentrations below 10<sup>-11</sup> M compared to higher concentrations.<sup>36</sup> One important implication for this observation is that actinide  $K_d$ s at the ultralow concentrations (10<sup>-12</sup>–10<sup>-16</sup> M) found in the environment may differ from  $K_d$ s generated at the concentrations used in typical laboratory experiments ( $\geq 10^{-10}$  [Pu]  $\leq 10^{-6}$  M). Although a primary assumption of reactive transport models, the validity of extrapolating Pu sorption behavior from relatively high concentration laboratory experiments to the low concentrations found in many field settings has not been rigorously tested.

The principal aim of the current study was to investigate the adsorption of Pu(V) to montmorillonite in experiments that spanned both typical laboratory and environmental concentrations (10<sup>-6</sup> to 10<sup>-16</sup> M). In order to examine Pu sorption over 10 orders of magnitude of concentration, three different analytical techniques were used: accelerator mass spectrometry (AMS), inductively coupled plasma mass spectrometry (ICP-MS), and liquid scintillation counting (LSC). The use of AMS allowed us to perform adsorption studies at unprecedented, low Pu concentrations (10<sup>-15</sup> to 10<sup>-16</sup> M), which are representative of environmental concentrations. Second, differences in the adsorption behavior of Pu(IV) and Pu(V) to montmorillonite were examined. The third aim was to compare the sorption

rates of Pu(V) to a variety of environmentally relevant mineral phases using both data from the literature as well as data from experiments performed in our lab. This study highlights the importance of oxidation state in controlling Pu sorption, the likely importance of redox active species within mineral phases in controlling surface mediated reduction rates, and the uniquely slow apparent sorption rates that result when obvious redox active species are not present in a mineral phase.

## MATERIALS AND METHODS

**Montmorillonite Preparation.** Unless stated otherwise, all solutions were prepared using ultrapure water (Milli-Q Gradient System, >18 M $\Omega$ .cm) and ACS grade chemicals without further purification. Details regarding the preparation of SWy-1 montmorillonite (Source Clays Repository of the Clay Minerals Society) for use in sorption experiments have been reported previously.<sup>13</sup> Briefly, the montmorillonite was treated with 0.001 M HCl and 0.03 M H<sub>2</sub>O<sub>2</sub> to remove soluble salts and minimize the oxidation/reduction capacity of any impurities. The clay was then homo-ionized in 0.01 M NaCl solution and dialyzed in MQ H<sub>2</sub>O to remove excess salts. The homo-ionized clay was centrifuged at 180 g for 5 min and 2500 g for 6 h to remove the >2  $\mu$ m and <50 nm particles from the suspension. The suspension was then dried at 40 °C. A portion of the dried montmorillonite was resuspended in a 0.7 mM NaHCO<sub>3</sub>, 5 mM NaCl buffer solution (pH 8) to make a suspension with a montmorillonite concentration of  $\sim 10$  g kg<sup>-1</sup>. The stock solution was allowed to equilibrate for several days prior to the start of sorption experiments.

A small portion of the dried montmorillonite was lightly ground and used for a surface area measurement (N<sub>2</sub>(g)-BET Quadrasorb SI). The particles had a surface area of 31.5  $\pm$  0.17 m<sup>2</sup> g<sup>-1</sup>, consistent with the reported value of 31.8  $\pm$  0.22 m<sup>2</sup> g<sup>-1</sup> (Clay Minerals Repository). The XRD pattern (Bruker D8 X-ray diffractometer) matched the montmorillonite reference pattern from the International Centre for Diffraction Data. No other mineral phases were observed indicating that the prepared montmorillonite was ostensibly pure. The amount of 0.5 N HCl extractable Fe was found to be 9.5  $\pm$  0.6  $\times 10^{-6}$  mol<sub>Fe</sub> g<sup>-1</sup><sub>clay</sub> by the method of Lovley and Phillips.<sup>37</sup>

**Plutonium Batch Sorption Experiments.** Sorption experiments were performed over a wide range of initial Pu concentrations (10<sup>-6</sup>–10<sup>-16</sup> M). In the following description we use the nominal terms *high concentration* to refer to experiments initially spiked to Pu concentrations of 10<sup>-6</sup>–10<sup>-11</sup> M and *low concentration* for experiments initially spiked to Pu concentrations of 10<sup>-12</sup>–10<sup>-16</sup> M. The two types of experiments were performed in separate laboratories in order to minimize any potential contamination of the *low concentration* samples.

**Pu Stock Solutions.** A <sup>242</sup>Pu stock (15.8% <sup>238</sup>Pu, 5.1% <sup>239+240</sup>Pu, 79.1% <sup>242</sup>Pu by activity) and a <sup>238</sup>Pu stock (98.8% <sup>238</sup>Pu, 0.11% <sup>241</sup>Pu, and 0.1% <sup>239</sup>Pu by activity) were used in the *high concentration* sorption experiments. A New Brunswick Laboratory (NBL) Pu reference material CRM-137 (33.5% <sup>238</sup>Pu, 35.3% <sup>239</sup>Pu, 31.3% <sup>240</sup>Pu by activity) was used in the *low concentration* sorption experiments. Three different stock solutions were used in order to facilitate measurement of the wide range of Pu concentrations used in the experiments via the three techniques described below. The Pu stock solutions were purified using anion exchange resin (BioRad AG 1  $\times$  8, 100–200 mesh). The Pu concentration was determined by both LSC (Packard Tri-Carb TR2900 LSA and Ultima Gold cocktail) and ICP-MS (XSeries II, Thermo Scientific) using <sup>233</sup>U as an internal standard.

Pu oxidation states in the stock solutions were manipulated by heating in 1 M HCl to produce Pu(IV) and heating in concentrated HNO<sub>3</sub> followed by adjustment to pH 3 with NaOH and heating with 0.05 M hydrogen peroxide to produce Pu(V). Pu oxidation states were determined using LaF<sub>3</sub> coprecipitation and solvent extraction techniques, as described in the Supporting Information (SI).<sup>13</sup> We note that minor variations in the purity of each oxidation state in the various stocks did exist but did not appear to affect sorption data.

**Sorption Experiments.** All Pu(IV) and Pu(V) batch sorption experiments were performed under air in 0.7 mM NaHCO<sub>3</sub>, 5 mM NaCl buffer solution (pH 8) with 1 g L<sup>-1</sup> montmorillonite. Pu(IV)

and Pu(V) aqueous speciation for initial Pu concentrations of  $10^{-10}$  M in the buffer solution were calculated using the Geochemist's Workbench family of codes and thermodynamic data from Guillaumont et al. (2003).<sup>38</sup> The results are shown in SI Figure S1. Batch experiments were conducted in either 50 mL Nalgene Oak Ridge polycarbonate centrifuge tubes (*high concentration*) or 500 mL Nalgene polycarbonate bottles (*low concentration*). Higher volumes were required in *low concentration* experiments to achieve the low detection limits afforded by AMS. Pu(V) sorption experiments were performed at *low concentrations* and *high concentrations*, while Pu(IV) experiments were performed only at *high concentrations*. For Pu(IV) experiments, where the stock solution was in 1 M HCl, NaOH was added to the samples immediately prior to spiking in order to neutralize the acidity associated with the Pu(IV) spike. This was not necessary for Pu(V) experiments where the pH of the stock solution was 3. Montmorillonite blanks (with no Pu) and Pu spiked blanks (with no montmorillonite) were run in parallel. The pH of each experiment was checked (Orion 920A with calibrated electrode) and adjusted to  $\text{pH } 8.0 \pm 0.2$  using dilute NaOH or HCl within 10 min of spiking. Typically, pH values remained within 0.2 units of the initial pH over 30 days. Samples were placed on an orbital shaker at 125 rpm at room temperature for the duration of the experiment. Samples were kept in the dark in order to minimize photocatalyzed reactions that may directly or indirectly affect the redox speciation of Pu.<sup>25,39</sup> To examine the differences in the rate of sorption between Pu(IV) and Pu(V) a series of time-dependent experiments were also performed at initial Pu concentrations of  $10^{-6}$  M and  $10^{-9}$  M.

To quantify the experimental errors involved in sorption experiments, systems with an initial concentration of  $10^{-11}$  M were run in quadruplicate. The standard deviation at the  $1\sigma$  level after a 30 day sorption period was used as an estimate of experimental error for all samples.

At each time point, samples were centrifuged to achieve a 50 nm size cut off. Tests performed with 3 kD ultrafiltration devices (Nanosep 3K Omega; approximate metric size discrimination: 1 nm) demonstrated that there was no difference in Pu concentration between the supernatant and the ultrafiltered supernatant (SI Figure S2). In *high concentration* experiments, aliquots of the supernatant were removed and counted via LSC or removed and acidified to 2%  $\text{HNO}_3$  for analysis via ICP-MS. In *low concentration* experiments, aliquots of supernatant were acidified to 2%  $\text{HNO}_3$  and analyzed using AMS (10-MeV tandem accelerator at the Center for Accelerator Mass Spectrometry (CAMS), Lawrence Livermore National Laboratory, CA). AMS is an ultrasensitive analytical technique that can quantify long-lived radionuclides at ultralow concentrations and routinely achieves instrumental backgrounds of  $10^5$  atoms for actinide elements.<sup>40</sup> AMS analysis has been reported previously and included isotope dilution using a nonisobarically interfering isotope of  $^{242}\text{Pu}$  (99.99%  $^{242}\text{Pu}$ ).<sup>40</sup>

## RESULTS AND DISCUSSION

**Sorption Rates of Pu to Montmorillonite.** The rate of Pu(IV) and Pu(V) sorption to montmorillonite was studied using initial concentrations of  $10^{-6}$  and  $10^{-9}$  M Pu for each oxidation state (Figure 1). The majority of Pu(IV) was sorbed within the first hour (95% and 80% of  $10^{-6}$  and  $10^{-9}$  M Pu, respectively). At both concentrations, sorption continued after the first hour, but at a much slower rate, for the remainder of the 30 day experiment. In contrast, Pu(V) sorption was initially much slower: only 15% and 10% of Pu was removed in the  $10^{-6}$  and  $10^{-9}$  M experiments, respectively, after 1 h. Pu(V) also continued to sorb to the montmorillonite for the 30 day duration of the experiment. An initial fast rate of uptake followed by a slower approach to equilibrium is a common feature of previous time-dependent studies of Pu sorption to other inorganic minerals.<sup>6,12,13,30,41</sup> Differences in Pu(IV) and Pu(V) sorption kinetics have previously been observed on goethite and calcite and attributed to a rate controlling surface

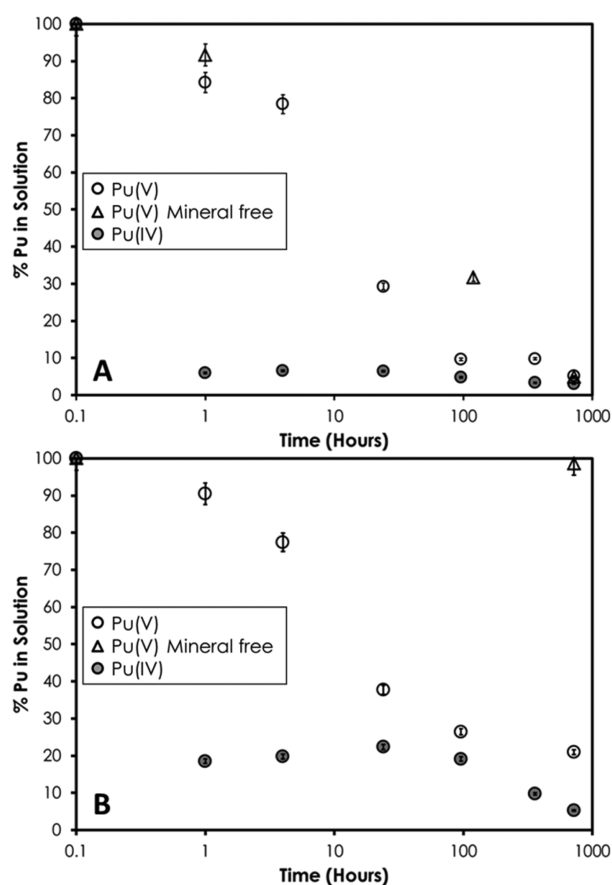


**Figure 1.** Sorption of Pu(IV) (closed circles) and Pu(V) (open circles) to SWy-1 Na-montmorillonite plotted as percentage of Pu removed from solution vs time. The behavior of Pu(V) in mineral-free systems is plotted for comparison (triangles). Initial Pu concentrations were (A)  $10^{-6}$  M and (B)  $10^{-9}$  M. A  $t = 0$  value of 0.1 h is used to facilitate plotting on a log time scale which is necessary given the fast removal of Pu(IV) from solution. Error bars calculated as described in the Materials and Methods section.

mediated reduction of Pu(V) to Pu(IV).<sup>6,42</sup> Thus, the slower sorption in the Pu(V) systems compared to the Pu(IV) systems is likely due to the slow reduction of Pu(V) on the montmorillonite surface. Similarly, the period of slow sorption observed in our Pu(IV) data is most probably an artifact of the slow sorption of Pu(V) impurities in the stock solution. The predicted aqueous speciation of representative Pu(IV) and Pu(V) experiments ( $[\text{Pu}] 10^{-10}$  M) shows that Pu(IV) will most likely be present as  $\text{Pu}(\text{OH})_4$  in solution with carbonate species unlikely to be important (SI Figure S1). In contrast, as much as 30% of Pu(V) may be present as  $\text{PuO}_2\text{CO}_3^-$  with the majority of Pu(V) present as  $\text{PuO}_2^+$  at pH 8. Thus, it is possible that carbonate species will impact both the adsorption of Pu(V) and reduction of adsorbed Pu(V) species. Unfortunately the impact of carbonate species was not further investigated, as solution conditions were kept constant to allow for comparison between Pu(V) and Pu(IV) species over the range of concentrations investigated. However, previous work has indicated that total alkalinity values  $>100$  meq  $\text{L}^{-1}$  are needed for there to be a significant impact on adsorption of Pu(V) and this is much greater than the total alkalinity used in the current study ( $<1$  meq  $\text{L}^{-1}$ ).<sup>6</sup>

In the absence of montmorillonite, removal of  $10^{-9}$  M Pu(V) from solution was minimal ( $<3\%$ ), indicating that sorption to

container walls is insignificant for this oxidation state and concentration. However, the removal of  $10^{-6}$  M Pu(V) from solution in the absence of montmorillonite after 120 h is about 70%. In a similar but separate mineral-free Pu(V) sorption experiment, both the bulk solution Pu and the supernatant Pu were monitored as a function of time (SI Figure S3B). Based on these data and reported Pu(V) solubility limits for natural waters at circumneutral pH ( $\sim 10^{-6}$  M –  $\sim 10^{-9}$  M) the loss of Pu from the montmorillonite-free bulk solution at  $10^{-6}$  M Pu is most likely attributed to sorption and/or precipitation of Pu to the vial walls although we are unable to speculate further on the exact nature of this Pu.<sup>11,20,43</sup> In a second parallel experiment performed in the presence of montmorillonite, loss of Pu activity from the bulk suspension was minimal while the supernatant concentration decreased substantially (SI Figure S3A). This indicates that the majority of Pu removed from solution is associated with montmorillonite rather than the container walls when the mineral is present. Thus, it is important to note that at high concentrations, surface precipitation of Pu may be contributing to the removal of Pu from solution in mineral containing systems, as will be discussed in the context of the sorption isotherm below.

**Pu-Montmorillonite Isotherm.** The sorption of Pu(V) to montmorillonite was studied over an initial Pu(V) concentration range of  $10^{-6}$ – $10^{-16}$  M. After 30 days of equilibration, the Pu(V) sorption isotherm is linear over this wide range of initial Pu concentrations (Figure 2). Importantly, this linearity

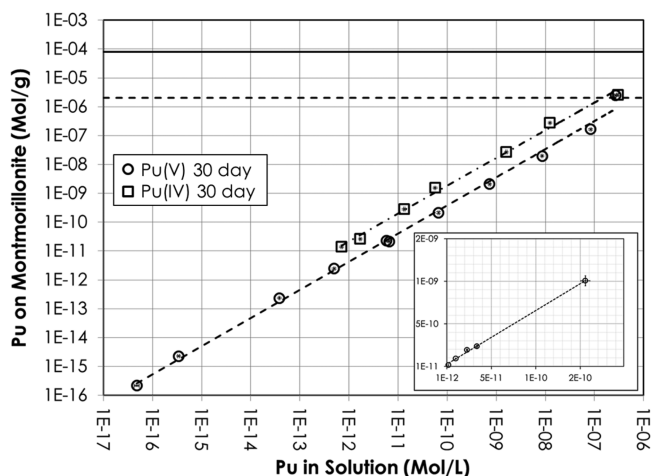


**Figure 2.** 30 day Pu(V) (circles) and 30 day high concentration Pu(IV) (squares) sorption isotherms for SWy-1 Na-montmorillonite ( $1 \text{ g L}^{-1}$ ) in  $0.7 \text{ mM NaHCO}_3$ ,  $5 \text{ mM NaCl}$  buffer solution at pH 8. Included on the plot are estimated strong site (horizontal dashed line) and weak site (horizontal full line) concentrations for SWy-1 Na-montmorillonite.<sup>44</sup> Inset shows higher density data on a linear plot for comparison. Error bars calculated as described in the Materials and Methods section.

suggests that Pu–surface interactions on montmorillonite at typical laboratory concentrations ( $\geq 10^{-10}$  [Pu]  $\leq 10^{-6}$  M) are broadly similar to those operating at ultralow environmental concentrations. The similarity in behavior is observed despite the different Pu stock solutions used in the experiments and small differences in the initial oxidation state of the stock solutions. A separate isotherm with a narrower range of initial Pu concentrations ( $10^{-9}$ – $10^{-11}$  M) but higher data density was used to test whether data density across this wide concentration range masks any nonlinear behavior and is shown on a linear

plot (Figure 2, inset). These data lead to the same linear behavior as observed in the bulk Pu(V) isotherm, indicating that the log–log plot does not mask major deviations in the adsorption data.

Although the overall trend for the Pu(V) sorption isotherm is linear, there is a noticeable deviation from linearity for the highest concentration data-point (Figure 2). The solubility of Pu(V) has been reported to vary from  $\sim 10^{-6}$  M to  $\sim 10^{-9}$  in natural waters at circumneutral pH depending on the experimental setup and the solubility limiting species.<sup>10,11,20,43</sup> Thus, as has been discussed previously, the highest Pu concentration used in this work ( $\sim 10^{-6}$  M) may exceed the solubility limit of Pu(V) under the current experimental conditions. Therefore, in this system it is likely that surface precipitation on the clay surface (or bulk precipitation followed by association with the clay surface) is occurring in addition to adsorption. Further evidence that precipitation is occurring at  $10^{-6}$  M is shown in SI Figure S4. This plot shows time-series data for sorption experiments performed with diaspore ( $\alpha\text{-AlOOH}$ ), as well as the montmorillonite time-series data, at initial Pu(V) concentrations ranging from  $10^{-6}$  M to  $10^{-9}$  M. The weak affinity of Pu(V) for diaspore at  $10^{-9}$  and  $10^{-8}$  M Pu (below expected Pu(V) solubility) is in contrast to the apparent strong sorption at  $10^{-6}$  M. Thus, the data for Pu(V) sorption to diaspore further demonstrates the potential for enhanced removal of Pu caused by surface precipitation.

The slope of the Pu(V) isotherm is  $0.98 \pm 0.02$  ( $r^2 = 0.998$ ) on the log–log plot (Figure 2). Given the closeness of this slope to unity, sorption can be considered linear and Langmuirian in behavior. However, unlike traditional Langmuir plots which exhibit a flattening of the isotherm as mineral surface sites become saturated, the data remain linear at higher concentrations, even perhaps steepening as the solubility limit of Pu is reached. Previously, Bradbury and Baeyens estimated strong site and weak site concentrations for SWy-1 Na-montmorillonite of  $2 \times 10^{-3}$  and  $8 \times 10^{-2} \text{ mol kg}^{-1}$ , respectively, and these values have been used in subsequent modeling studies.<sup>34,44–46</sup> In Figure 2 we have included these maximum strong site and weak site concentrations. Plotting these concentrations demonstrates that saturation of strong sites is only achieved in the sample containing  $10^{-6}$  M Pu. Given that this sample shows signs of surface precipitation, it is perhaps not surprising that flattening of the isotherm is not observed: the effect of strong site saturation (i.e., reduced uptake of Pu) is masked by the fact that surface precipitation of Pu likely occurs at this concentration. Furthermore, under these conditions, the existence of a weak site is not relevant since precipitation will surely occur before any significant contribution of the weak site is observed. Importantly, the linear sorption behavior observed here is consistent with the two site model of Bradbury and Baeyens, since in the case of Pu, precipitation at high concentration masks any possible nonlinearity associated with the second site.<sup>45</sup>

In contrast to changes in adsorption behavior at high adsorbate concentration as a result of surface site saturation, recent work by Snow et al. has highlighted that changes in adsorption behavior for Np may occur at ultralow concentrations.<sup>36,47</sup> In the work of Snow et al., a change in Np(V) sorption affinity for goethite was demonstrated by a marked change in the slope of the adsorption isotherm at Np concentrations below  $10^{-11}$  M and was attributed to the presence of a unique, low density adsorption site.<sup>36</sup> This behavior contrasts with the apparent linear behavior in the case

of Pu adsorption to montmorillonite observed in the present work.

$K_d$  values for Pu(V) sorption to montmorillonite ranged from 1970 mL g<sup>-1</sup> to 9100 mL g<sup>-1</sup>. However, this upper value is the value for the 10<sup>-6</sup> M system so likely includes a solubility limited component, as discussed previously. Excluding this value returns a  $K_d$  range of 1970–6700 mL g<sup>-1</sup>. This range compares favorably with work by Runde et al. who reported a  $K_d$  value for Pu(V) sorption on montmorillonite of 5800 mL g<sup>-1</sup> at pH 6.9 after a 10 day equilibration and Lu et al. who obtained a value of ~10<sup>4</sup> mL g<sup>-1</sup> in Pu(V) montmorillonite colloid experiments at pH 8.2–8.3 after a 21 day equilibration.<sup>30,43</sup> Interestingly, in the present study, there is a trend toward slightly lower  $K_d$  values as the aqueous Pu concentration increases, but this difference is insufficient to warrant speculation about the existence of an adsorption site with a marginally higher sorption affinity for Pu at low Pu concentrations.

High concentration Pu(IV) sorption experiments were run in parallel to the Pu(V) experiments. The Pu(IV) sorption isotherm at 30 days also demonstrates linear behavior with a slope of 0.96 ± 0.03 ( $r^2 = 0.995$ ) (Figure 2). However, while the slope is the same, within error, to that observed for the Pu(V) data, the Pu(IV) sorption data exhibit a greater sorption affinity for the montmorillonite surface at this time point. This difference in behavior is consistent with the Pu time series data, where Pu(IV) sorption is greater and more rapid than Pu(V) over a 30 day time scale (Figure 1).

The high concentration Pu(V) sorption experiments were resampled after 330 days (Figure 3). After almost a year, the

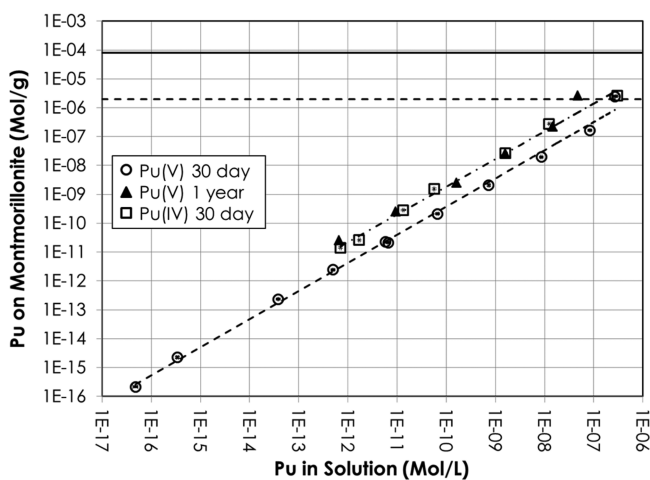


**Figure 3.** 30 day Pu(V) (circles), 30 day high concentration Pu(IV) (squares), and 1 year high concentration Pu(V) (triangles) sorption isotherms for SWy-1 Na-montmorillonite (1 g L<sup>-1</sup>) in 0.7 mM NaHCO<sub>3</sub>, 5 mM NaCl buffer solution at pH 8. Error bars calculated as described in the Materials and Methods section.

high concentration Pu(V) data isotherm retains its linearity (log–log slope = 0.98 ± 0.06;  $r^2 = 0.984$ ). However, continued sorption of Pu(V) over this period means that the isotherm has shifted toward the Pu(IV) 30 day isotherm data. Further, continued sorption demonstrates that the Pu(V) sorption process did not reach equilibrium after 30 days. In the mineral free Pu(V) system at 10<sup>-9</sup> M, there was a 13% decline in solution concentration over this one year time scale, as compared with 78–90% in mineral containing systems. This

confirms that sorption of Pu to the montmorillonite surface is responsible for the continued slow removal of Pu(V) from solution.

Given that the slope of the Pu(V) data at high concentrations remains unchanged, that it is similar to the slope of the Pu(IV) data, and that the Pu(V) isotherm moves toward the Pu(IV) isotherm after one year of equilibration, we conclude that the relative sorption of Pu to montmorillonite in these experiments is not only independent of initial Pu concentration but also independent of initial oxidation state over long enough time periods. Importantly, the approach to equilibrium is very slow. A slow approach to equilibrium has previously been predicted and observed for Pu(V) adsorption to montmorillonite and is attributed to the continued reduction of Pu(V) on the mineral surface.<sup>13,30</sup> Thus, in the present work, we suggest that the eventual similarity in Pu(V) and Pu(IV) adsorption to montmorillonite is due to the slow reduction of Pu(V) to Pu(IV) on the mineral surface which leads to similar Pu oxidation state distributions on the montmorillonite. Importantly, these Pu(V), and to a lesser extent Pu(IV), data highlight that the time scales needed to achieve thermodynamic equilibrium in systems containing complex minerals and redox-active species may be on the orders of months to years, in contrast to typical adsorption experiments which are performed on the scale of days to weeks.<sup>6,26,30,43</sup>

If slow reduction of Pu(V) to Pu(IV) is responsible for the continued removal of Pu from solution, it is interesting to consider the processes responsible for the reduction of Pu(V). Previous suggestions for Pu reduction mechanisms in the presence of mineral phases include Pu(V) disproportionation, the presence of a reductant such as Fe(II), electron shuttling in certain oxide phases, and self-reduction by  $\alpha$  particle induced radiolysis products.<sup>25,27,48,49</sup> Also, a previous study has demonstrated that Pu(V) reduction to Pu(IV) on montmorillonite may be facilitated by H<sup>+</sup> exchange sites.<sup>13</sup>

Self-reduction and disproportionation mechanisms at the trace Pu concentrations used in the majority of these experiments are unlikely and have recently been ruled out by Romanachuk et al., while the alkaline pH value (pH 8) used in the current work means that reduction at H<sup>+</sup> exchange sites is unlikely to be a significant mechanism.<sup>48</sup> The presence of Fe species within clay has been used to explain the reduction of Pu(V) by sediments from the Savannah River Site, SC.<sup>49</sup> Despite initial attempts to remove free Fe from the clay used in our experiments, structural Fe will nonetheless remain.<sup>50</sup> The 0.5 N HCl extractable content of the treated clay was 9.5 × 10<sup>-6</sup> mol<sub>Fe</sub> g<sup>-1</sup><sub>clay</sub>. With the solid:solution ratio of 1 g L<sup>-1</sup> montmorillonite used in these experiments, there is likely sufficient Fe in the montmorillonite to reduce all of the Pu(V) present (i.e., there is a 3-fold excess of Fe compared to Pu(V) at the highest Pu(V) concentration used in these experiments). Although we do not know the oxidation state of the structural Fe present in the montmorillonite, a recent study of SWy-2 Na-montmorillonite (from the same location as SWy-1) demonstrated that all of the structural iron present in the clay was redox active.<sup>51</sup> Thus in the present work, reduction by redox active structural iron in the montmorillonite could be a viable mechanism for the slow reduction of Pu(V) on the clay surface.

**Comparison of Apparent Pu Sorption Rates.** In order to highlight the importance of mineralogy, and in particular the importance of redox-active species in controlling Pu sorption rates, we examined the apparent rates of Pu(V) sorption to a variety of minerals. Apparent first order sorption rate constants

are commonly obtained by calculating the slope of the linear portion (far from equilibrium) of a plot of  $\ln(C)$  versus time.<sup>13</sup> However, this is difficult to achieve when adsorption is rapid and/or when experimental data are sparse. One approach to overcoming these limitations is to fit the adsorption data with a simple first order model containing terms for a forward adsorption rate constant and a reverse desorption rate constant. By surface area normalizing the forward rate, we can generate a consistent, yet qualitative value that allows us to compare rates across a wide range of mineral data (details provided in SI) as well as data from previously published studies. Calculated rate constants from this study were compared to unpublished pH 8 rate data from our laboratory for Pu(V) sorption to groutite ( $\alpha$ -MnOOH), goethite ( $\alpha$ -FeOOH), diaspore ( $\alpha$ -AlOOH), corundum ( $\alpha$ -Al<sub>2</sub>O<sub>3</sub>), gibbsite (Al(OH)<sub>3</sub>), and high purity quartz (SiO<sub>2</sub>) as well as previously published sorption rate data for Pu(V) sorption to hematite ( $\alpha$ -Fe<sub>2</sub>O<sub>3</sub>), goethite ( $\alpha$ -FeOOH), and magnetite (Fe<sub>3</sub>O<sub>4</sub>) at pH 8.<sup>12,25</sup>

A plot of the log of the apparent sorption rate constants for these various mineral phases against the initial concentration of Pu used in each experiment is shown in Figure 4. There is a

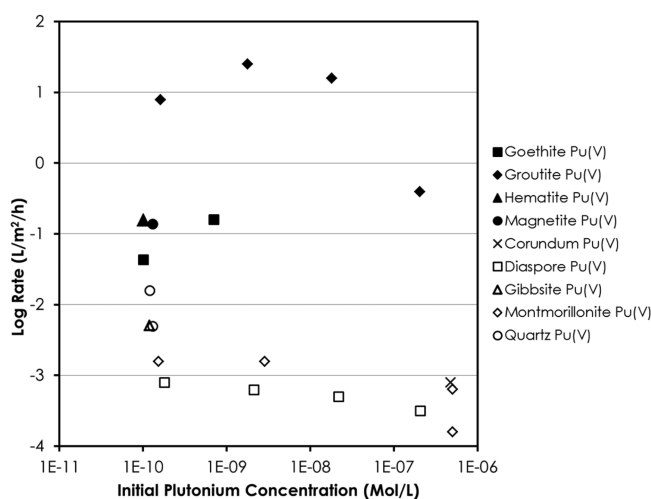


**Figure 4.** Surface area normalized apparent adsorption rates for Pu(V) on different mineral phases plotted as a function of initial Pu(V) concentration. Data from this study, except magnetite data at 10<sup>-10</sup> M from Powell et al. (2004), and goethite and hematite data at 10<sup>-10</sup> M taken from Powell et al. (2005).<sup>12,25</sup>

clear difference in the Pu(V) sorption rate constants for Fe/Mn containing mineral phases (goethite, groutite, hematite, magnetite) versus mineral phases with little or no Fe/Mn (corundum, diaspore, gibbsite, montmorillonite, quartz). The rate constant for quartz is higher than other non Fe/Mn containing minerals yet still lower than the Fe/Mn mineral rates. This is consistent with the findings of Lu et al. who observed that sorption rates for Pu(V) followed the trend hematite > silica > montmorillonite.<sup>30</sup> Although the mineral point of zero charge (p.z.c.) likely plays a role in the uptake of Pu(V) and may account for the faster rate seen in the case of quartz (see SI Table S1), the lack of correlation between p.z.c. and apparent sorption rate suggests that surface charge effects play a secondary role in Pu(V) uptake. Previous studies have demonstrated that Fe oxyhydroxides can effectively reduce Pu(V) to Pu(IV) on the mineral surface.<sup>6,12,18,25,26,52</sup> Similarly, although the redox behavior of Mn oxyhydroxides is somewhat more complicated, rapid Pu reduction has been observed in the

presence of Mn(II) and Mn(III) bearing minerals.<sup>27,41,53,54</sup> Thus, for the minerals compared here, it would appear that the presence of a mineral phase with the ability to effect rapid reduction of Pu(V) (i.e., a redox active component) contributes to higher apparent sorption rates. However, in the case of montmorillonite, it seems that either the low concentration of Fe present limits the rate of reduction of Pu(V) to Pu(IV) compared to the pure Mn/Fe containing minerals or the structural Fe does not effect the reduction of Pu(V). The former conclusion is consistent with the findings of Hixon et al. who found that rates of Pu reduction by clay minerals were correlated with the Fe(II) content of the clays.<sup>49</sup> The latter observation suggests that there may be other processes causing reduction/slow uptake of Pu(V) from solution by montmorillonite.

The comparison of apparent adsorption rate constants highlights the likely importance of Pu(V) reduction to Pu(IV) in controlling the uptake of Pu(V) from solution in the environment and further demonstrates the key role which Fe/Mn containing minerals are likely to play in this process. Together with the observations from the adsorption isotherms, the rate data demonstrates the importance of both long-term adsorption studies and desorption experiments to fully describe environmental systems where multiple processes, such as redox transformations, sorption affinities and sorption/desorption rates are expected to control the rate, extent, and permanency of Pu uptake.

## ■ ASSOCIATED CONTENT

### 📄 Supporting Information

**Materials and Methods:** Pu aqueous speciation, ultracentrifugation data, Pu oxidation state analysis. **Results and Discussion:** Comparison of Pu concentrations in bulk suspension and supernatant, plutonium solubility, parallel adsorption rate experiments. This material is available free of charge via the Internet at <http://pubs.acs.org>.

## ■ AUTHOR INFORMATION

### Corresponding Author

\*E-mail: [begg2@llnl.gov](mailto:begg2@llnl.gov).

### Notes

The authors declare no competing financial interest.

## ■ ACKNOWLEDGMENTS

We would like to thank Rachel Lindvall for help with ICP-MS analysis and the anonymous reviewers for their constructive criticism which greatly improved this manuscript. This work was supported by the Subsurface Biogeochemical Research Program of the U.S. Department of Energy's Office of Biological and Environmental Research. Prepared by LLNL under Contract DE-AC52-07NA27344.

## ■ REFERENCES

- (1) Nelson, D. M.; Lovett, M. B. Oxidation state of plutonium in the Irish Sea. *Nature* **1978**, *276* (5688), 599–601.
- (2) Montero, P. R.; Sanchez, A. M. Plutonium contamination from accidental release or simply fallout: study of soils at Palomares (Spain). *J. Environ. Radioactiv.* **2001**, *55* (2), 157–165.
- (3) Smith, D. K.; Finnegan, D. L.; Bowen, S. M. An inventory of long-lived radionuclides residual from underground nuclear testing at the Nevada test site, 1951–1992. *J. Environ. Radioactiv.* **2003**, *67* (1), 35–51.

- (4) Morris, K.; Butterworth, J. C.; Livens, F. R. Evidence for the remobilization of Sellafield waste radionuclides in an intertidal salt marsh, West Cumbria, UK. *Estuarine, Coastal Shelf Sci.* **2000**, *51* (5), 613–625.
- (5) EPA, *Drinking water regulations and health advisories*; Environmental Protection Agency, Washington, DC, 1996; p 23
- (6) Sanchez, A. L.; Murray, J. W.; Sibley, T. H. The adsorption of plutonium IV and plutonium V on goethite. *Geochim. Cosmochim. Acta* **1985**, *49* (11), 2297–2307.
- (7) Choppin, G. R. Redox speciation of plutonium in natural waters. *J. Radioanal. Nucl. Chem.* **1991**, *147* (1), 109–116.
- (8) Kersting, A. B.; Efurud, D. W.; Finnegan, D. L.; Rokop, D. J.; Smith, D. K.; Thompson, J. L. Migration of plutonium in ground water at the Nevada Test Site. *Nature* **1999**, *397* (6714), 56–59.
- (9) Novikov, A. P.; Kalmykov, S. N.; Utsunomiya, S.; Ewing, R. C.; Horreard, F.; Merkulov, A.; Clark, S. B.; Tkachev, V. V.; Myasoedov, B. F. Colloid transport of plutonium in the far-field of the Mayak Production Association, Russia. *Science* **2006**, *314* (5799), 638–641.
- (10) Efurud, D. W.; Runde, W.; Banar, J. C.; Janecky, D. R.; Kaszuba, J. P.; Palmer, P. D.; Roensch, F. R.; Tait, C. D. Neptunium and plutonium solubilities in a Yucca Mountain groundwater. *Environ. Sci. Technol.* **1998**, *32* (24), 3893–3900.
- (11) Neck, V.; Altmairer, M.; Seibert, A.; Yun, J. I.; Marquardt, C. M.; Fanghanel, T. Solubility and redox reactions of Pu(IV) hydrous oxide: Evidence for the formation of PuO<sub>2+x</sub>(s, hyd). *Radiochim. Acta* **2007**, *95* (4), 193–207.
- (12) Powell, B. A.; Fjeld, R. A.; Kaplan, D. I.; Coates, J. T.; Serkiz, S. M. Pu(V)O<sub>2</sub><sup>+</sup> adsorption and reduction by synthetic magnetite (Fe<sub>3</sub>O<sub>4</sub>). *Environ. Sci. Technol.* **2004**, *38* (22), 6016–6024.
- (13) Zavarin, M.; Powell, B. A.; Bourbin, M.; Zhao, P. H.; Kersting, A. B. Np(V) and Pu(V) ion exchange and surface-mediated reduction mechanisms on montmorillonite. *Environ. Sci. Technol.* **2012**, *46* (5), 2692–2698.
- (14) Icopini, G. A.; Lack, J. G.; Hersman, L. E.; Neu, M. P.; Boukhalfa, H. Plutonium(V/VI) reduction by the metal-reducing Bacteria *Geobacter metallireducens* GS-15 and *Shewanella oneidensis* MR-1. *Appl. Environ. Microbiol.* **2009**, *75* (11), 3641–3647.
- (15) Zhao, P. H.; Zavarin, M.; Leif, R. N.; Powell, B. A.; Singleton, M. J.; Lindvall, R. E.; Kersting, A. B. Mobilization of actinides by dissolved organic compounds at the Nevada Test Site. *Appl. Geochem.* **2011**, *26* (3), 308–318.
- (16) Santschi, P. H.; Roberts, K. A.; Guo, L. D. Organic nature of colloidal actinides transported in surface water environments. *Environ. Sci. Technol.* **2002**, *36* (17), 3711–3719.
- (17) Powell, B. A.; Dai, Z. R.; Zavarin, M.; Zhao, P. H.; Kersting, A. B. Stabilization of plutonium nano-colloids by epitaxial distortion on mineral surfaces. *Environ. Sci. Technol.* **2011**, *45* (7), 2698–2703.
- (18) Kirsch, R.; Fellhauer, D.; Altmairer, M.; Neck, V.; Rossberg, A.; Fanghanel, T.; Charlet, L.; Scheinost, A. C. Oxidation state and local structure of plutonium reacted with magnetite, mackinawite, and chukanovite. *Environ. Sci. Technol.* **2011**, *45* (17), 7267–7274.
- (19) Felmy, A. R.; Moore, D. A.; Rosso, K. M.; Qafoku, O.; Rai, D.; Buck, E. C.; Ilton, E. S. Heterogeneous reduction of PuO<sub>2</sub> with Fe(II): Importance of the Fe(III) reaction product. *Environ. Sci. Technol.* **2011**, *45* (9), 3952–3958.
- (20) Nitsche, H.; Edelstein, N. M. Solubilities and speciation of selected transuranium ions. A comparison of a non-complexing solution with a groundwater from the Nevada Tuff Site. *Radiochim. Acta* **1985**, *39* (1), 23–33.
- (21) Silva, R. J.; Nitsche, H. Actinide environmental chemistry. *Radiochim. Acta* **1995**, *70–1*, 377–396.
- (22) Choppin, G. R. Actinide speciation in the environment. *J. Radioanal. Nucl. Chem.* **2007**, *273* (3), 695–703.
- (23) Orlandini, K. A.; Penrose, W. R.; Nelson, D. M. Pu(V) as the stable form of oxidized plutonium in natural waters. *Mar. Chem.* **1986**, *18* (1), 49–57.
- (24) Kaplan, D. I.; Powell, B. A.; Duff, M. C.; Demirkanli, D. I.; Denham, M.; Fjeld, R. A.; Molz, F. J. Influence of sources on plutonium mobility and oxidation state transformations in vadose zone sediments. *Environ. Sci. Technol.* **2007**, *41* (21), 7417–7423.
- (25) Powell, B. A.; Fjeld, R. A.; Kaplan, D. I.; Coates, J. T.; Serkiz, S. M. Pu(V)O<sub>2</sub><sup>+</sup> adsorption and reduction by synthetic hematite and goethite. *Environ. Sci. Technol.* **2005**, *39* (7), 2107–2114.
- (26) Keeney-Kennicutt, W. L.; Morse, J. W. The redox chemistry of Pu(V)O<sub>2</sub><sup>+</sup> interaction with common mineral surfaces in dilute solutions and seawater. *Geochim. Cosmochim. Acta* **1985**, *49* (12), 2577–2588.
- (27) Powell, B. A.; Duff, M. C.; Kaplan, D. I.; Fjeld, R. A.; Newville, M.; Hunter, D. B.; Bertsch, P. M.; Coates, J. T.; Eng, P.; Rivers, M. L.; Sutton, S. R.; Triay, I. R.; Vaniman, D. T. Plutonium oxidation and subsequent reduction by Mn(IV) minerals in Yucca Mountain tuff. *Environ. Sci. Technol.* **2006**, *40* (11), 3508–3514.
- (28) Sabodina, M. N.; Kalmykov, S. N.; Sapozhnikov, Y. A.; Zakharova, E. V. Neptunium, plutonium and <sup>137</sup>Cs sorption by bentonite clays and their speciation in pore waters. *J. Radioanal. Nucl. Chem.* **2006**, *270* (2), 349–355.
- (29) Lujanienė, G.; Motiejunas, S.; Sapolaite, J. Sorption of Cs, Pu and Am on clay minerals. *J. Radioanal. Nucl. Chem.* **2007**, *274* (2), 345–353.
- (30) Lu, N. P.; Reimus, P. W.; Parker, G. R.; Conca, J. L.; Triay, I. R. Sorption kinetics and impact of temperature, ionic strength and colloid concentration on the adsorption of plutonium-239 by inorganic colloids. *Radiochim. Acta* **2003**, *91* (12), 713–720.
- (31) Vaniman, D.; Furlano, A.; Chipera, S.; Thompson, J.; Triay, I. Microautoradiography in studies of Pu(V) sorption by trace and fracture minerals in tuff. *MRS Proceedings* **1995**, *412*, 639–646.
- (32) Dzombak, D. A.; Morel, F. M. M., *Surface complexation modeling: hydrous ferric oxide*; Wiley-Interscience: New York, 1993; p 393.
- (33) McKinley, J. P.; Zachara, J. M.; Smith, S. C.; Turner, G. D. The influence of uranyl hydrolysis and multiple site-binding reactions on adsorption of U(VI) to montmorillonite. *Clay Clay Miner.* **1995**, *43* (5), 586–598.
- (34) Kraepiel, A. M. L.; Keller, K.; Morel, F. M. M. A model for metal adsorption on montmorillonite. *J. Colloid Interface Sci.* **1999**, *210* (1), 43–54.
- (35) Benjamin, M. M.; Leckie, J. O. Multiple-site adsorption of Cd, Cu, Zn, and Pb on amorphous iron oxyhydroxide. *J. Colloid Interface Sci.* **1981**, *79* (1), 209–221.
- (36) Snow, M. S.; Zhao, P. H.; Dai, Z. R.; Kersting, A. B.; Zavarin, M. Neptunium(V) sorption to goethite at attomolar to micromolar concentrations using radiometric methods. *J. Colloid Interface Sci.* **2013**, *390*, 176–182.
- (37) Lovley, D. R.; Phillips, E. J. P. Availability of ferric iron for microbial reduction in bottom sediments of the freshwater tidal Potomac River. *Appl. Environ. Microbiol.* **1986**, *52* (4), 751–757.
- (38) Guillaumont, R.; Fanghanel, T.; Neck, V.; Fuger, J.; Palmer, D. A.; Grenthe, I.; Rand, M. H. *Update on the chemical thermodynamics of uranium, neptunium, plutonium, americium, and technetium*; Elsevier: Amsterdam, 2003; Vol. 5.
- (39) McCubbin, D.; Leonard, K. S. Photochemical dissolution of radionuclides from marine sediments. *Mar. Chem.* **1996**, *55*, 399–408.
- (40) Marchetti, A. A.; Brown, T. A.; Cox, C. C.; Hamilton, T. F.; Martinelli, R. E. Accelerator mass spectrometry of actinides. *J. Radioanal. Nucl. Chem.* **2005**, *263* (2), 483–487.
- (41) Shaughnessy, D. A.; Nitsche, H.; Booth, C. H.; Shuh, D. K.; Waychunas, G. A.; Wilson, R. E.; Gill, H.; Cantrell, K. J.; Serne, R. J. Molecular interfacial reactions between Pu(VI) and manganese oxide minerals Manganite and hausmannite. *Environ. Sci. Technol.* **2003**, *37* (15), 3367–3374.
- (42) Zavarin, M.; Roberts, S. K.; Hakem, N.; Sawvel, A. M.; Kersting, A. B. Eu(III), Sm(III), Np(V), Pu(V), and Pu(IV) sorption to calcite. *Radiochim. Acta* **2005**, *93* (2), 93–102.
- (43) Runde, W.; Conradson, S. D.; Efurud, D. W.; Lu, N. P.; VanPelt, C. E.; Tait, C. D. Solubility and sorption of redox-sensitive radionuclides (Np, Pu) in J-13 water from the Yucca Mountain site:

comparison between experiment and theory. *Appl. Geochem.* **2002**, *17* (6), 837–853.

(44) Baeyens, B.; Bradbury, M. H. A mechanistic description of Ni and Zn sorption on Na-montmorillonite Part I: Titration and sorption measurements. *J. Contam. Hydrol.* **1997**, *27* (3–4), 199–222.

(45) Bradbury, M. H.; Baeyens, B. A mechanistic description of Ni and Zn sorption on Na-montmorillonite Part II: Modelling. *J. Contam. Hydrol.* **1997**, *27* (3–4), 223–248.

(46) Bradbury, M. H.; Baeyens, B. Modelling the sorption of Mn(II), Co(II), Ni(II), Zn(II), Cd(II), Eu(III), Am(III), Sn(IV), Th(IV), Np(V) and U(VI) on montmorillonite: Linear free energy relationships and estimates of surface binding constants for some selected heavy metals and actinides. *Geochim. Cosmochim. Acta* **2005**, *69* (4), 875–892.

(47) Tinnacher, R. M.; Zavarin, M.; Powell, B. A.; Kersting, A. B. Kinetics of neptunium(V) sorption and desorption on goethite: An experimental and modeling study. *Geochim. Cosmochim. Acta* **2011**, *75* (21), 6584–6599.

(48) Romanchuk, A. Y.; Kalmykov, S. N.; Aliev, R. A. Plutonium sorption onto hematite colloids at femto- and nanomolar concentrations. *Radiochim. Acta* **2011**, *99* (3), 137–144.

(49) Hixon, A. E.; Hu, Y. J.; Kaplan, D. I.; Kukkadapu, R. K.; Nitsche, H.; Qafoku, O.; Powell, B. A. Influence of iron redox transformations on plutonium sorption to sediments. *Radiochim. Acta* **2010**, *98* (9–11), 685–692.

(50) Van Olphen, H.; Fripiat, J. J. *Data handbook for clay materials and other non-metallic minerals*; Pergamon Press: Oxford, 1979; p 346.

(51) Gorski, C. A.; Klüpfel, L.; Voegelin, A.; Sander, M.; Hofstetter, T. B. Redox properties of structural Fe in clay minerals. 2. Electrochemical and spectroscopic characterization of electron transfer irreversibility in ferruginous smectite, SWa-1. *Environ. Sci. Technol.* **2012**, *46* (17), 9369–9377.

(52) Penrose, W. R.; Metta, D. N.; Hyklo, J. M.; Rinckel, L. A. Chemical speciation of plutonium in natural waters. *J. Environ. Radioact.* **1987**, *5*, 169–184.

(53) Morgenstern, A.; Choppin, G. R. Kinetics of the oxidation of Pu(IV) by manganese dioxide. *Radiochim. Acta* **2002**, *90*, 69–4.

(54) Duff, M. C.; Hunter, D. B.; Triay, I. R.; Bertsch, P. M.; Reed, D. T.; Sutton, S. R.; Shea-Mccarthy, G.; Kitten, J.; Eng, P.; Chipera, S. J.; Vaniman, D. T. Mineral associations and average oxidation states of sorbed Pu on tuff. *Environ. Sci. Technol.* **1999**, *33* (13), 2163–2169.